PCCP

Accepted Manuscript

This is an *Accepted Manuscript*, which has been through the Royal Society of Chemistry peer review process and has been accepted for publication.

Accepted Manuscripts are published online shortly after acceptance, before technical editing, formatting and proof reading. Using this free service, authors can make their results available to the community, in citable form, before we publish the edited article. We will replace this *Accepted Manuscript* with the edited and formatted *Advance Article* as soon as it is available.

You can find more information about *Accepted Manuscripts* in the Information for Authors.

Please note that technical editing may introduce minor changes to the text and/or graphics, which may alter content. The journal's standard Terms & Conditions and the Ethical guidelines still apply. In no event shall the Royal Society of Chemistry be held responsible for any errors or omissions in this *Accepted Manuscript* or any consequences arising from the use of any information it contains.

ROYAL SOCIETY OF CHEMISTRY

www.rsc.org/pccp

Tunable electronic and magnetic properties of monolayer MoS_2 on decorated AlN nanosheets: A van der Waals density functional study

C. He[1,*], W. X. Zhang[2,*], T. Li[2], L. Zhao[2], X. G. Wang[2]

[1] *State Key Laboratory for Mechanical Behavior of Materials, School of Materials Science and Engineering, Xi'an Jiaotong University, Xi'an 710049, China*

[2] *School of Materials Science and Engineering, Chang'an University, Xi'an 710064, China*

Abstract

In this paper, the structural, electronic, and magnetic properties of monolayer MoS_2 on decorated AlN nanosheets have been systematically investigated on density functional theory with van der Waals corrections. The results indicate that the surface microstructure of AlN substrate and stacking patterns significantly affect the electronic and magnetic properties of heterostructures. Moreover, *n* type semiconductor → *p* type semiconductor → metal transition accompanied with nonmagnetic → magnetic transfer can be achieved for monolayer MoS_2. The diverse electronic and magnetic properties highlight MoS_2 nanosheets potential applications in electronics and spintronics.

* Corresponding Authors: C. He (hecheng@mail.xjtu.edu.cn) or W. X. Zhang (wxzhang@chd.edu.cn)

Physical Chemistry Chemical Physics Accepted Manuscript

1. Introduction

In recent years, stimulated by the isolation of graphene from graphite, two-dimensional (2D) crystal wholly refreshed our minds and brought us a new revolution to material science due to its extraordinary structural and electronic properties as well as promising applications in nanoelectronics.[1-4]

The impressive progress in graphene research has motivated scientists to explore other 2D atomic based materials. Among them, Molybdenum disulfide (MoS_2), a hexagonal crystal structure, is constructed by the S-Mo-S monolayer (sandwiched structure with a Mo layer coupled by two S layers) through van der Waals interaction.[5-8] Such a unique structure endows MoS_2 many excellent thermal, electric, optical and mechanical properties[9-17] and at the same time provides sufficient interlayer spaces for intercalating foreign molecules and atoms.[18-20] Unlike its bulk counterpart, the monolayer MoS_2 is a direct gap semiconductor with a finite bandgap of 1.8 eV by virtue of the quantum size effect and can be a promising candidate for logic devices due to the significant bandgap,[21] relatively high carrier mobility and high ON/OFF ratio.[22-26]

Many experimental and simulation studies have predicted that monolayer MoS_2 could be an interesting material for future applications in nanoelectronics.[26-30] Moreover, it has been reported that the bandgap of MoS_2 changes from indirect to direct when the thickness is reduced to monolayer.[31,32] The indirect - to - direct gap transition of MoS_2 sparks off great enhancement in photoresponse.[33] Recently, low-cost photodetectors composed of liquid-exfoliated MoS_2 nanosheets have been fabricated.[34]

Physical Chemistry Chemical Physics Accepted Manuscript

Nevertheless, some important issues remain largely unexplored, for example, how to choose a suitable substrate; and how to control the *n*- or *p*- type conductivity nature of MoS_2. Some semiconducting substrates have been proposed theoretically, such as SiO_2,[35] *h*-BN,[5] *p*-type Si,[36] graphene,[37] ZnO (0001)[38] and other plastic surfaces for nanoelectronic devices.

Therefore, we suggest a new substrate, decorated AlN nanosheets, for monolayer MoS_2 based on the perfect match of the lattice constant of these two materials. Such heterostructures are proposed partly because of the similar lattice constants, i.e. 3.14 Å for monolayer MoS_2 [38] and 3.112 Å for hydrogen-functionalized AlN,[39] respectively. Meanwhile, AlN nanosheet, as another kind of 2D atomic based material, has become a hotly pursued system as it shares the same honeycomb lattice structure as graphene. AlN nanosheet has aroused extensive research interests due to its many intriguing properties such as high chemical stabilities, excellent mechanical properties and high thermal conductivity.[40,41] Unlike graphene, the surface Al and N atoms in AlN nanosheet have different reacting and bonding natures with H atoms.[39]

Thus, as a substrate, fully and partially hydrogenated AlN nanosheets are suitable choice. Therefore, it would be of great importance to understand how decorated AlN nanosheets affect the electronic and magnetic properties of monolayer MoS_2. In addition, Van der Waals (vdW) heterostructures have been widely synthesized and led to a great deal of experimentally and theoretically studies.[42-45] Most recently, Georgiou *et al.* have proposed that the creation of the heterostructures assembling two different 2D crystals

Physical Chemistry Chemical Physics Accepted Manuscript

into three-dimensional stacks with atomic layer precision is an important milestone in the post-silicon electronic era.[46]

Therefore, in the following, the structural, electronic and magnetic properties of MoS_2 on fully and partially hydrogenated AlN nanosheets are extensively carried out by density functional theory (DFT) calculations with vdW corrections. These studies provide us a deep understanding of the novel properties of monolayer MoS_2, which is essential to enrich them for future nanodevices.

2. Computational methods

The simulations are based on density functional theory (DFT), which is provided by DMOL^3. [47-49] The generalized gradient approximation (GGA) with the Perdew-Burke-Ernzerhof scheme (PBE) [50] is adopted for the exchange-correlation potential to optimize geometrical structures and calculate properties for both spin-polarized and spin-unpolarized case.[51] In order to take into account the contributions of the van der Waals (vdW) interactions between different layers, the DFT-D (D stands for dispersion) approach within the Grimme scheme is adopted for the vdW correction.[52] This method has been successfully applied in previous studies of the interaction between silicene on MoS_2 [53] and benzene on Cu (100) surfaces.[54] DFT Semi-core Pseudopots (DSPP), which induce some degree of relativistic correction into the core, are used for the core treatment. Moreover, double numerical atomic orbital plus polarization (DNP) is chosen as the basis set, with the global orbital cutoff 4.4 Å. Similar functional have been successfully used to study the structural and electronic properties of GNRs, Si and Cu nanowires.[51,56,57] The nearest distance between nanosheets in neighboring cells is greater than 15 Å to ensure no interactions between different layers. For geometry optimization,

Physical Chemistry Chemical Physics Accepted Manuscript

both the cell and the atomic positions are allowed to fully relax. The Brillouin zone is sampled by 6 × 6 × 1 (10 × 10 × 1) *k*-points for all structures in the geometry optimization (electronic) calculations, which brings out the convergence tolerance of energy of 1.0×10^{-5} Ha (1 Ha = 27.2114 eV), maximum force of 0.002 Ha/Å, and maximum displacement of 0.005 Å. Increasing the *k*-points mesh to 8× 8 × 1 for all structures in the geometry optimization does not greatly change the calculated quantities. It is believed that the numerical basic sets implemented in $DMol^3$ could minimize or even eliminate basis set superposition error (BSSE), compared with Gaussian basis sets.[59] Since $DMol^3$ uses the exact DFT spherical atomic orbitals, the molecules can be dissociated exactly into their constituent atoms. Consequently, the corrections of BSSE are not considered here.

The electronic distributions of heterostructures are carried out by Mulliken charge analysis, which are performed using a projection of a Linear Combination of Atomic Orbitals (LCAO) basis and to specify quantities such as atomic charge, bond population, charge transfer etc. LCAO supplies better information regarding the localization of the electrons in different atomic layers than a plane wave basis set does.[57] The obtained relative values of the charge *e*, but not the absolute magnitude, display a high degree of sensitivity to the atomic basis set and a relative distribution of charge.[58]

The formation energy (E_f), which is to evaluate the structural stability of the heterostructure systems, is defined as: $E_f = E_{\text{heterostructure}} - E_{\text{MoS}_2} - E_{\text{substrate}}$, where $E_{\text{heterostructure}}$ is the energy of the heterostructure system, E_{MoS_2} is the energy of the free standing MoS_2 and $E_{\text{substrate}}$ is the energy of the decorated AlN nanosheet substrate.[53,54]

Physical Chemistry Chemical Physics Accepted Manuscript

According to this definition, the negative values of E_f implies bounded systems; the smaller the value, the energetically stronger heterostructure system binding.

3. Results and discussion

The accuracy of our calculation procedure is tested by monolayer MoS_2. The full relaxed lattice constant of monolayer MoS_2 is 3.168 Å, which agrees well with other theoretical results (3.14-3.183 Å).[38,53] A 4 × 4 × 1 supercell of monolayer MoS_2 nanosheet containing 48 atoms is constructed (Fig. 1a). The calculated direct band gap (E_g) of 1.85 eV (Fig. 1b) is also in good agreement with previous theoretical results (1.8-1.9 eV) [38,53] and experimental data.[22, 60] The Mulliken charge analysis results indicate that the same atoms are equivalent and $e_S = -0.067\ e$ and $e_{Mo} = 0.134\ e$.

Similar to Zn and O sites in ZnO nanosheets, Al and N sites in AlN nanosheets are chemically nonequivalent, and then semi-hydrogenation can be achieved by merely saturating either all the Al sites or all the N sites. In this study, three decorated AlN nanosheets configurations with lattice constant of 3.112 Å are considered: fully hydrogenated AlN nanosheet (H-AlN-H), semi-hydrogenation with H on N sites (denoted as AlN-H), and semi-hydrogenation with H on Al sites (denoted as H-AlN), which are discussed in our previous study.[39] In addition, comparing the total energy of the spin-polarized and spin-unpolarized states, the electronic and magnetic properties of three decorated AlN systems are also calculated.[39]

Note that the matched structure usually forms when the mismatch between lattice constants is small.[53] Being similar to the modeling methods of silicene - silicon [45] and

Physical Chemistry Chemical Physics Accepted Manuscript

silicene - MoS_2 [53] heterostructures, we constructed the heterostructures of monolayer MoS_2 on the top of the decorated AlN nanosheets. We chose the lattice constant of the monolayer MoS_2 (12.672 Å), and scaled the in-plane lattice constant of decorated AlN nanosheets, resulting in a reasonably small mismatch of around 1.76%.

In this work, there are 12 initial heterostructures assembled by monolayer MoS_2 and single-layer H-AlN-H to find out the optimal stacking manners between these two 2D crystals. In detail, the MoS_2 supercell is firstly fixed. Then the H-AlN-H supercell is moved along *x*-axis or *y*-axis. Thus, three representative stacking patterns are formed: Top structure (sulfur atoms situated directly above Al atoms, short for T_S and Molybdenum atoms situated directly above Al atoms short for T_{Mo}); Bridge structure (sulfur atoms located at the top of the mid-points of Al and N, short for B_S and Molybdenum atoms located at the top of the mid-points of Al and N, short for B_{Mo}); Hollow structure (sulfur atoms placed at the hollow sites of the N-Al-N hexagonal rings, short for H_S and Molybdenum atoms placed at the hollow sites of the N-Al-N hexagonal rings, short for H_{Mo}) are considered, which are shown in Fig. 2a-f. In addition, the location of Al atom and N atom are exchanged. Thus, about $6 \times 2 = 12$ configurations are constructed as the initial stacking manners and the corresponding structural parameters are calculated. The structural parameters and E_g values for different patterns are similar, which is in agreement with the silicene - silicon [45] and silicene - MoS_2 [53] heterostructures. Thus, in the following, we only consider the most stable configuration in Fig. 2f, which has a characteristic that sulfur atoms are placed at the hollow site of the N-Al-N

Physical Chemistry Chemical Physics Accepted Manuscript

hexagonal rings.

DFT-D2 includes vdW contributions using a semiempirical potential added to the total DFT energy.[53,54] We therefore have evaluated the performance of this method in the first system of our study (MoS_2/H-AlN-H) as follows (see Fig. 2g). The interlayer distance d_0 means the nearest distance between monolayer MoS_2 and the H-AlN-H substrate. With vdW, we included the contribution of the dispersion forces in the whole system, while without vdW correction, dispersion forces have been partially considered.

Fig. 2g shows the cohesive energy of MoS_2/H-AlN-H as a function of interlayer distance d_0 using the DFT-D2 method, which illustrates that the H_S stacking has a distinctly energy minima at 2.19 Å, a typical distance for chemisorption.[43] In the heterostructure system, the average intraplanar bond lengths are 1.940 Å and 2.443 Å for $d_{Al\text{-}N}$ and $d_{S\text{-}Mo}$, respectively. The Al and N atoms become sp^3 hybridized with H atoms bonded, which distorts the planar geometry forming a zigzag configuration. The optimized Al-H bond lengths (1.581 Å) and N-H bond lengths (1.035 Å) indicate the formation of strong chemical bonds between hydrogen and Al, N atoms.[39]

Although both DFT and DFT-D2 calculations indicate that MoS_2 can stably be attached on H-AlN-H without any energy barriers (Fig. 2g), the pure DFT method without vdW correction fails to give a stable adsorption state. Specifically, there is no well-defined minimum in the cohesive-energy curve, and the cohesive energy is significantly underestimated compared to the vdW-inclusive results. Therefore, the

Physical Chemistry Chemical Physics Accepted Manuscript

interaction distance vs Energy curve is quite different from DFT+D result and shows the importance of a correct use of the vdW correction.

To evaluate the structural stability of the MoS_2/H-AlN-H heterostructure, we calculated the formation energies, which are listed in Table 1. According to this definition, a system with smaller E_f value is more favorable. The DFT-D2 formation energy (-0.865 eV) for the configuration shown in Fig. 2f exhibits that the MoS_2/H-AlN-H heterostructure is thermodynamically stable since no imaginary frequency appears from the phonon analysis.[43]

It was reported that the electronic properties of graphene related materials are modulated notably by weak interlayer interactions.[45,53] To reveal this effect on MoS_2, the electronic structure of MoS_2/H-AlN-H heterostructure is shown in Fig. 3. The MoS_2/H-AlN-H heterostructure is nonmagnetic semiconductor with the indirect band gap of 1.72 eV. Compared with the band structures of monolayer MoS_2 and the fully hydrogenated one-bilayer nanosheet (H-AlN-H),[39] obviously, E_g value of heterostructure decreases from 1.85 eV of isolated monolayer MoS_2 and a direct- to - indirect gap transition occurs, as expected on the basis of the relatively weak interlayer interactions.

In order to see the states near the E_F, the partial density of states (PDOS) of the separated MoS_2 and H-AlN-H from the heterostructure are plotted in Fig. 3. It is found that the states of MoS_2/H-AlN-H near the E_F are mainly dominated by the bands in MoS_2, denoting that the electronic and transport behaviors of the hybrid structure are mainly determined by the MoS_2 monolayer. Moreover, in order to gain more insights into the

Physical Chemistry Chemical Physics Accepted Manuscript

electronic structure of MoS_2/H-AlN-H system, the corresponding charge density isosurfaces of the lowest unoccupied molecular orbital (LUMO) and the highest occupied molecular orbital (HOMO) at Gamma point have been explored, where E_g of this system is determined by the two subbands. LUMO orbitals are primarily localized on the Mo atoms, while for HOMO orbitals, the charge densities are homogeneously distribute over the whole MoS_2 monolayer, which are corresponding to our previous BS and PDOS results.

The Mulliken charge analysis[57] of MoS_2/H-AlN-H shown in Table 2 indicate that the average Mulliken populations of the S atoms at the outer and inner in MoS_2 are 0.02 *e* and 0.052 *e*, respectively, which means the electron densities are distributed unequally and the sublattice symmetry in MoS_2 is broken. Furthermore, atomic charge transfers (Q_T) from monolayer MoS_2 to H-AlN-H nanosheet are analyzed to understand the nature of the interaction[45] and the corresponding results are shown in Table 1. The Mulliken population analysis shows that monolayer MoS_2 accepts total 0.105 $|e|$ from the H-AlN-H substrate, leading to *n*-doping MoS_2.

Similarly, we also investigate the electronic and magnetic properties monolayer MoS_2 on semi-hydrogenation on Al sites or N sites of AlN nanosheet, which denote as MoS_2/AlN-H and MoS_2/H-AlN, respectively. The most stable structure is also searched through three kinds of representative stacking patterns (Top structure, Bridge structure, and Hollow structure).

Physical Chemistry Chemical Physics Accepted Manuscript

In Fig. 4, we summarize the results of the MoS_2/AlN-H heterostructure. The most stable stacking structure is Hollow structure H_{Mo} as shown in Fig. 4a, which is formed by placing Molybdenum atoms at the hollow sites of the N-Al-N hexagonal rings. Interestingly, the system prefers the ferromagnetic ground state. The origin of the magnetic behavior is further investigated by plotting the spin density distribution ($\Delta\rho = \rho_{up} - \rho_{down}$) in Fig. 4c. Obviously, the emergent spin polarization is not only restricted to the surface Al atoms but also is delocalized uniformly in the Mo atoms, leading to a net magnetic moment of approximately 1.148 μ_B per unit cell. The magnetic moment at every Al atom is about 0.185 μB and the rest magnetic moment mainly comes from the spin-polarized Mo atoms (0.083 μB). Moreover, MoS_2/AlN-H heterostructure is strikingly metallic and the induced metallicity is attributed to the partially occupied surface state of AlN-H, which is not completely removed after hydrogen passivation. Moreover, both of the electronic distribution for HOMO and LUMO orbitals continuously distribute over the whole system (Fig. 4d-e).

While for the MoS_2/H-AlN heterostructure, the most stable stacking structure is Top structure T_S, which is formed by placing sulfur atoms directly above Al atoms (Fig. 5a). As described in Fig. 5b, the MoS_2/H-AlN heterostructure behaves as a direct semiconductor and the values of E_g of 0.831 and 0.218 eV in the spin-up and spin-down states, respectively. The absorption of H atom on Al sites introduces a low acceptor level located slightly above the VBM, which is spin-polarized with only one spin channel completely occupied, resulting in hole-doping *p*-type conductivity. The spin polarization

Physical Chemistry Chemical Physics Accepted Manuscript

is evident in the band structure and PDOS (Fig. 5b). The induced magnetism is attributed primarily to unsaturated N atoms (0.467 μB per atom) and H atoms (0.281 μB per atom) in Fig. 5c, which is corresponding to the results as found in *n*-H-AlN nanosheets.[39] The calculated magnetic moment is 3.95 μB per unit cell for the MoS_2/H-AlN heterostructure. Thus, the MoS_2/H-AlN heterostructure possesses an essentially larger magnetic moment than the MoS_2/AlN-H heterostructure. This is easily understandable that the dangling bonds on Al atoms (as in AlN-H) exhibit much less spin density compared with those of unpaired N atoms (as in H-AlN).

Moreover, in order to gain more insights into the electronic structure of MoS_2/H-AlN system, the corresponding charge density isosurfaces of LUMO and HOMO orbitals at Gamma point have been explored in Fig. 5d and e. LUMO orbitals are primarily localized on the unpaired N atoms, while for HOMO orbitals, the charge densities are mainly attributed by the whole H-AlN monolayer and partly localized on the Mo atoms and the inner S atoms of MoS_2, which are corresponding to our previous BS and PDOS results.

The Mulliken charge analysis[57] of the MoS_2/AlN-H and MoS_2/H-AlN heterostructures are also shown in Table 2, which means the electron densities are distributed unequally and the sublattice symmetry in MoS_2 is also broken. The average Mulliken populations of the S atoms at the outer and inner in MoS_2/AlN-H (MoS_2/H-AlN) heterostructure are 0.096 *e* (0.054 *e*) and 0.286 *e* (0.043 *e*), respectively. Furthermore, atomic charge transfers (Q_T) shown in Table 1 show that MoS_2 monolayer donates total

Physical Chemistry Chemical Physics Accepted Manuscript

0.101 e to H-AlN substrate, leading to p-doping MoS_2. Comparing with the MoS_2 monolayer on fully hydrogenated AlN nanosheet substrate, the net values Q_T of MoS_2 on semi-hydrogenated AlN nanosheet substrates are much larger, which confirm that the electron transfers are accordingly accompanied with this strong adsorption effect. In addition, the charge transfer results are consistent with more negative E_f values that the interaction between the MoS_2/AlN-H (-1.533 eV) and MoS_2/H-AlN (-1.253 eV) heterostructures are much stronger than that of the MoS_2/H-AlN-H (-0.865 eV) heterostructure.[43]

4. Conclusions

In summary, we have systematically investigated the structural, electronic and magnetic properties of three heterostructures of monolayer MoS_2 on decorated AlN nanosheets by density functional theory with vdW corrections. The different hydrogenated sites on AlN substrates and stacking patterns significantly affect the electronic and magnetic properties of heterostructures. Our results predict that effectively controlling the hydrogenation sites and stacking patterns is a tunable way to modulate the properties of monolayer MoS_2. These intriguing and diverse properties of the novel heterostructures systems are of fundamental significance and open up exciting opportunities for the design of novel nanoelectronic spintronic devices.

Physical Chemistry Chemical Physics Accepted Manuscript

Acknowledgements

The authors acknowledge supports by National Natural Science Foundation of China (NSFC, nos. 51177006, 51301020 and 51471124), Natural Science Foundation of Shaanxi province, China (2014JQ6196), Ph.D. Programs Foundation of Ministry of Education of China (Grant no. 20110201120002), the special fund for basic scientific research of central colleges of Chang'an University (no. 2013G1311053) and National Training Programs of Innovation and Entrepreneurship for Undergraduates (no. 201310710064).

Physical Chemistry Chemical Physics Accepted Manuscript

References

1. Y. B. Zhang, Y. W. Tan, H. L. Stormer, and P. Kim, *Nature* 2005, **438**, 201.
2. K. S. Novoselov, Z. Jiang, Y. Zhang, S. V. Morozov, H. L. Stormer, U. Zeitler, J. C. Maan, G. S. Boebinger, P. Kim, and A. K. Geim, *Science* 2007, **315**, 1379.
3. C. Q. Sun, *Nanoscale*, 2010, **2**, 1930.
4. C. C. Yang, and S. Li, *J. Phys. Chem. B* 2009, **113**, 14207.
5. Z. Y. Huang, C. Y. He, X. Qi, H. Yang, W. L. Liu, X. L. Wei, X. Y. Peng, and J. X. Zhong, *J. Phys. D: Appl. Phys.* 2014, **47**, 075301.
6. D. Xiao, G. B. Liu, W. Feng, X. Xu, and W. Yao, *Phys. Rev. Lett.* 2012, **108**, 196802.
7. X. Song, J. Hu, and H. Zeng, *J. Mater. Chem. C* 2013, **1**, 2952.
8. Z. Huang, X. Peng, H. Yang, C. He, L. Xue, G. Hao, C. Zhang, W. Liu , X. Qi, and J. Zhong, *RSC Adv.* 2013, **3**, 12939.
9. S. F. Wu, J. S. Ross,G. B. Liu,G. Aivazian,A. Jones,Z. Y. Fei,W. G. Zhu,D. Xiao, W. Yao,D. Cobden, and X. D. Xu, *Nat. Phys.* 2013, **9**, 149.
10. H. L. Zeng, J. F. Dai, W. Yao, D. Xiao, and X. D. Cui, *Nat. Nanotechnol.* 2012, **7**, 490.
11. K. Roy, M. Padmanabhan, S. Goswami, T. P. Sai, G. Ramalingam, S. Raghavan, and A. Ghosh, *Nat. Nanotechnol.* 2013, **8**, 826.
12. L. Y. Li, and M. W. Zhao, *J. Phys. Chem. C*, 2014, **118**, 19129.
13. M. S. Fuhrer, and J. Hone, *Nat. Nanotechnol*. 2013, **8**, 146.
14. C. Martin, *Nat. Mater*. 2012, **11**, 829.
15. K. F. Mak, K. L. He, C. Lee, G. H. Lee, J. Hone, T. F. Heinz, and J. Shan, *Nat. Mater.* 2013, **12**, 207.
16. S. Kim, A. Konar, S. H. Wang, J. H. Lee, J. Lee, J. Yang, C. Jung, H. Kim, J. B. Yoo, J. Y. Choi, Y. W. Jin, S. Y. Lee, D. Jena, W. Choi, and K. Kim, *Nat. Commun.* 2012, **3**, 1011.
17. A. J. Groszek, *Nature* 1964, **204**, 680.

Physical Chemistry Chemical Physics Accepted Manuscript

18. M. Remškar, Z. Škraba, P. Stadelmann, and F. Lévy, *Adv. Mater.* 2000, **12**, 814.
19. J. Chen, N. Kuriyama, H. Yuan, H. T. Takeshita, and T. Sakai, *J. Am. Chem. Soc.* 2001, **123**, 11813.
20. Y. F. Li, D. H. Wu, Z. Zhou, R. Carlos Cabrera, and Z. F. Chen, *J. Phys. Chem. Lett.* 2012, **3**, 2221.
21. K. F. Mak, C. Lee, J. Hone, J. Shan, and T. F. Heinz, *Phys. Rev. Lett.* 2010, **105**, 136805.
22. B. Radisavljevic, A. Radenovic, J. Brivio, V. Giacometti, and A. Kis, *Nat. Nanotechnol.* 2011, **6**, 147.
23. Z. Yin, H. Li, L. Jiang, Y. Shi, Y. Sun, G. Lu, Q. Zhang, X. Chen, and H. Zhang, *ACS Nano*. 2012, **6**, 74.
24. H. Fang, S. Chuang, T. C. Chang, K. Takei, T. Takahashi, and A. Javey, *Nano Lett.* 2012, **12**, 3788.
25. Y. Li, C. Y. Xu,B. Y. Zhang, and L. Zhen, *Appl. Phys. Lett.* 2013, **103**, 033122.
26. J. Qi, X. Li, X. Qian, and J. Feng, *Appl. Phys. Lett*. 2013, **102**, 173112.
27. Q. H. Wang, K. Kalantar-Zadeh, A. Kis, J. N. Coleman and M. S. Strano, *Nature Nanotechnol*. 2012, **7**, 699.
28. M. Xu, T. Liang, M. Shi, and H. Chen, *Chem. Rev.* 2013, **113**, 3766.
29. Y. Yoon, K. Ganapathi, and S. Salahuddin, *Nano Lett*. 2011, **11**, 3768.
30. Z. Huang, G. Hao, C. He, H. Yang, L. Xue, X. Qi, X. Peng, and J. Zhong, *J. Appl. Phys.* 2013, **114**, 083706.
31. A. Splendiani, L. Sun, Y. Zhang, T. Li, J.Kim, C. Y. Chim, G. Galli, and F. Wang, *Nano. Lett*. 2010, **10**, 1271.
32. K. F. Mak, C. Lee, J. Hone, J. Shan, and T. F. Heinz, *Phys. Rev. Lett.* 2010, **105**, 136805.
33. O. Lopez-Sanchez, D. Lembke, M. Kayci, A. Radenovic, and A. Kis, 2013, **8**, 497.

Physical Chemistry Chemical Physics Accepted Manuscript

34. G. Cunningham, U. Khan, C. Backes, D. Hanlon, D. McCloskey, J. F. Donegan, and J.N.Coleman, *J. Mater. Chem.* 2013, **C1**, 6899.
35. B. Radisavljevic, A. Radenovic, J. Brivio, V. Giacometti, and A. Kis, *Nature Nanotechnol*. 2011, **6**, 147.
36. Y. J. Liu, L. Z. Hao, W. Gao, Q. Z. Xue, W. Y. Guo, Z. P. Wu, Y. L. Lin, H. Z. Zeng, J. Zhu, and W. L. Zhang, *J. Alloy. Compd.* 2015, **631**, 105.
37. N. G. Shang, P. Papakonstantinou, M. McMullan, M. Chu, A. Stamboulis, and A. Potenza, *Adv. Funct. Mater*.2008, **18**, 3506.
38. P. Liang, B. Tai, H. B. Shu, T. Shen, and Q. M. Dong, *Solid State Commun.* 2015, **204**, 67.
39. W. X. Zhang, T. Li, S. B. Gong, C. He, L. Duan, *Phys. Chem. Chem. Phys.*, 2015, **17**, 10919.
40. Y. Taniyasu, and M. Kasu, *Appl. Phys. Lett.* 2011, **98**, 131910.
41. P. Tsipas, S. Kassavetis, D. Tsoutsou, E. Xenogiannopoulou, E. Golias, S. A. Giamini, C. Grazianetti, D. Chiappe, A. Molle, M. Fanciulli, and A. Dimoulas, *Appl. Phys. Lett.* 2013, **103**, 251605.
42. A. K. Geim, and I. V. Grigorieva, *Nature* 2013, **499**, 419.
43. S. B. Tang, J. P. Yu, and L. X. Liu, *Phys. Chem. Chem. Phys.*2013, **15**, 5067.
44. T. H. Wang, Y. F. Zhu, and Q. Jiang, *J. Phys. Chem.*2013, *C***117**, 12873.
45. S. Li, Y. F. Wu, W. Liu, and Y. H. Zhao, *Chemi. Phys. Lett.* 2014, **609**, 161.
46. T. Georgiou, *Nature Nanotechnol*. 2013, **8**, 100.
47. H. Y. He, J. Hu, and B. C. Pan, *J. Chem. Phys.* 2009, **130**, 204516.
48. G. A. Gelves, B. Lin, U. Sundararaj, and J. A. Haber, *Adv. Funct. Mater.* 2006, **16**, 2423.
49. B. Delley, *J. Chem. Phys.* 1990, **92**, 508.
50. J. P. Perdew, K. Burke, and M. Ernzerhof, *Phys. Rev. Lett.* 1996, **77**, 3865.
51. Y. F. Zhu, Q. Q. Dai, M. Zhao, and Q. Jiang, *Sci. Rep.* 2013, **3**, 1524.

Physical Chemistry Chemical Physics Accepted Manuscript

52. S. Grimme, *J. Comput. Chem.* 2006, **27**, 1787.
53. N. Gao, J. C. Li and Q. Jiang, *Phys. Chem. Chem. Phys.* 2014, **16**, 11673.
54. M. Robledo, G. Pacchioni, F. Martín, M. Alcamí, and S. Díaz-Tendero, *J. Phys. Chem. C* 2015, **119**, 4062.
55. Z. M. Ao, and F. M. Peeters, *Appl. Phys. Lett.*, 2010, **96**, 253106.
56. R. Q. Zhang, W. T. Zheng, and Q. Jiang, *J. Phys. Chem. C* 2009, **113**, 10384.
57. C. He, P. Zhang, Y. F. Zhu, and Q. Jiang, *J. Phys. Chem. C* 2008, **112**, 9045.
58. E. R. Davidson, and S. Chakravorty, *Theor. Chim. Acta* 1992, **83**, 319.
59. Y. Inada, and H. Orita, *J. Comput. Chem.*, 2008, **29**, 225.
60. X. Q. Xie, Z. M. Ao, D. W. Su, J. Q. Zhang, G. X. Wang, *Adv. Functional Mater.* 2015, **25**, 1393.

Physical Chemistry Chemical Physics Accepted Manuscript

Table 1 Summary of the structural, electronic and magnetic properties of different heterostructures. d_0 means the nearest distance between monolayer MoS_2 and the decorated AlN substrates.

Type of interfacial microstructure	MoS_2/H-AlN-H		MoS_2/AlN-H		MoS_2/H-AlN	
Stable structure	H_S		H_{Mo}		T_S	
Bond type	Mo-S	Al-H	Mo-S	N-H	Mo-S	Al-H
Bond length (Å)	2.443	1.581	2.459	1.032	2.436	1.675
d_0 (Å)	2.19		2.28		2.41	
Q_T (e)	-0.105		0.255		0.101	
E_f (eV)	-0.865		-1.533		-1.253	
E_g (eV)	1.72		Metal		0.218	
Spin (hbar)	0		1.148		3.95	

Physical Chemistry Chemical Physics Accepted Manuscript

Table 2 Atom Mulliken charges of different heterostructures. The location of the sites is shown in Figs. 1, 4 and 5. The unit of charge is *e*.

Atom	MoS_2/H-AlN-H	MoS_2/AlN-H	MoS_2/H-AlN
Stable structure	H_S	H_{Mo}	T_S
S atom (Outer)	0.02	0.096	0.054
S atom (Inner)	0.052	0.286	0.043
Mo atom	-0.092	0.128	0.116
Al atom	0.823	1.027	0.987
N atom	-0.959	-0.952	-0.938
H atom (Outer)	0.189	0.180	0.063
H atom (Inner)	0.032	-	-

Physical Chemistry Chemical Physics Accepted Manuscript

Captions

Fig. 1. Optimized geometry (a) and the band structure (b) for 4 × 4 × 1 monolayer MoS_2. The yellow and green balls denote S and Mo atoms respectively. The supercell is represented by the green lines. Fermi level is set to zero.

Fig. 2. Side (top) and top (bottom) views of six atomic configurations for different stacking MoS_2/H-AlN-H heterostructures: (a) T_S; (b) T_{Mo}; (c) B_S; (d) B_{Mo}; (e) H_{Mo}; (f) H_S. (g) The adsorption results of different configurations as a function of interlayer distance between the two layers using DFT-D2 with vdW contribution and comparison of the adsorption results of H_S by DFT without vdW.

Fig. 3. The band structure, PDOS, charge densities of HOMO and LUMO at the Gamma point of MoS_2/H-AlN-H heterostructure as the stacking pattern H_S. PDOS results are also shown for selected orbitals. Blue and yellow denote positive and negative wave function contours in charge densities, respectively, and the isosurface values are ±0.025 e/$Å^3$.

Fig. 4. Optimized geometry, BS, PDOS, charge densities of LUMO and HOMO at the Gamma point, and the spin density distribution of MoS_2/AlN-H heterostructure as the stacking pattern H_{Mo}. Dark red surface corresponds to the isosurfaces of spin density with the isosurfaces of 0.01 e/$Å^3$.

Fig. 5. Optimized geometry, BS, PDOS, charge densities of LUMO and HOMO at the Gamma point, and the spin density distribution of MoS_2/H-AlN heterostructure as the stacking pattern T_S.

Physical Chemistry Chemical Physics Accepted Manuscript

Fig. 1

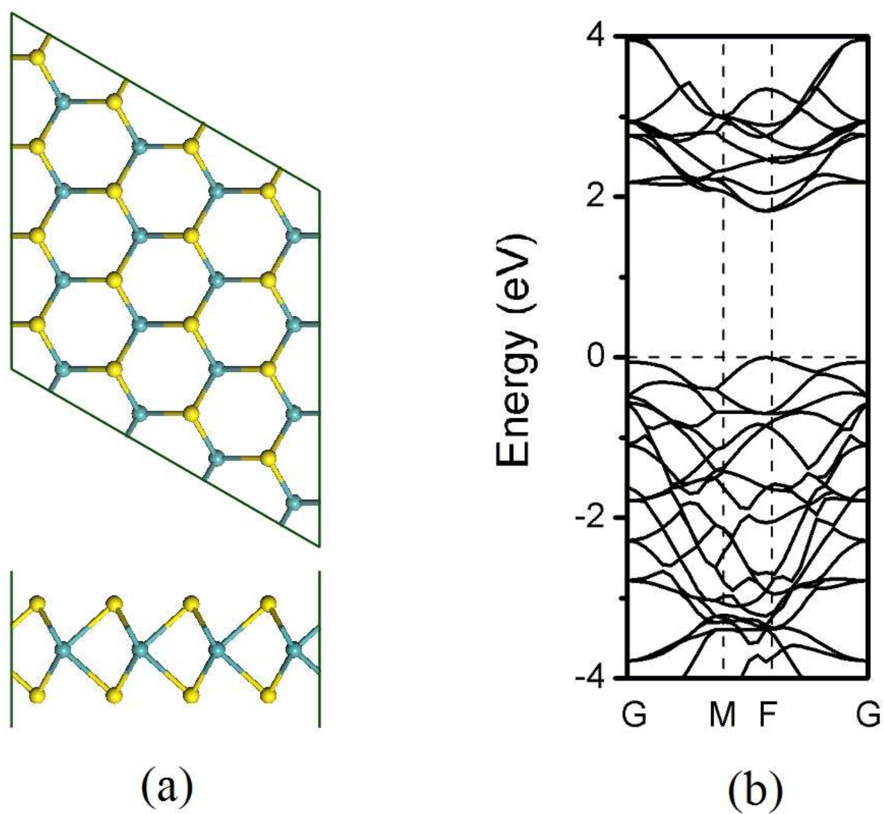

Physical Chemistry Chemical Physics Accepted Manuscript

Fig. 2

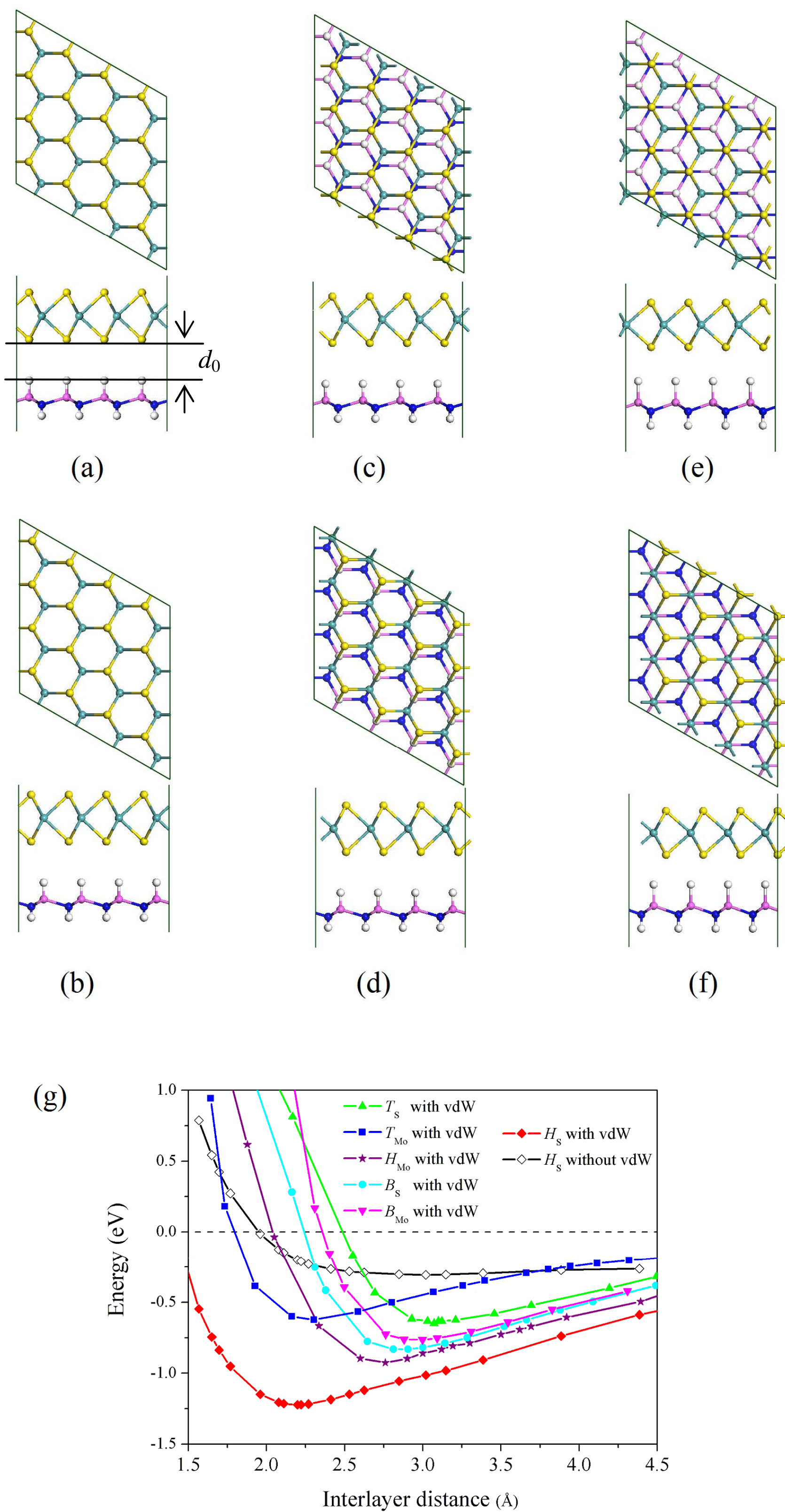

Physical Chemistry Chemical Physics Accepted Manuscript

Physical Chemistry Chemical Physics Accepted Manuscript

Fig. 3

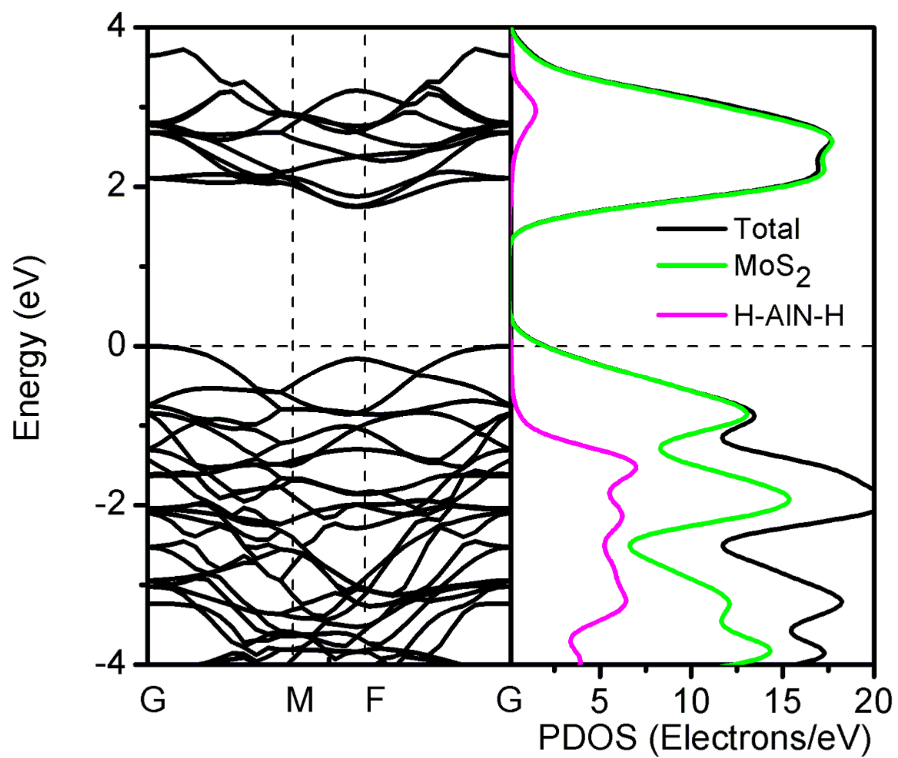

LUMO

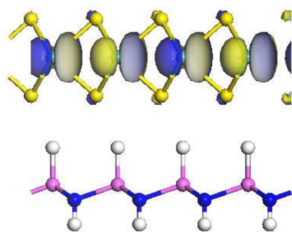

HOMO

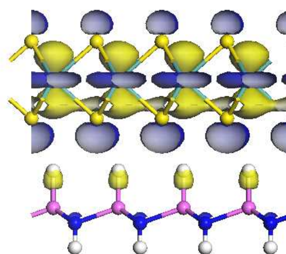

Fig. 4

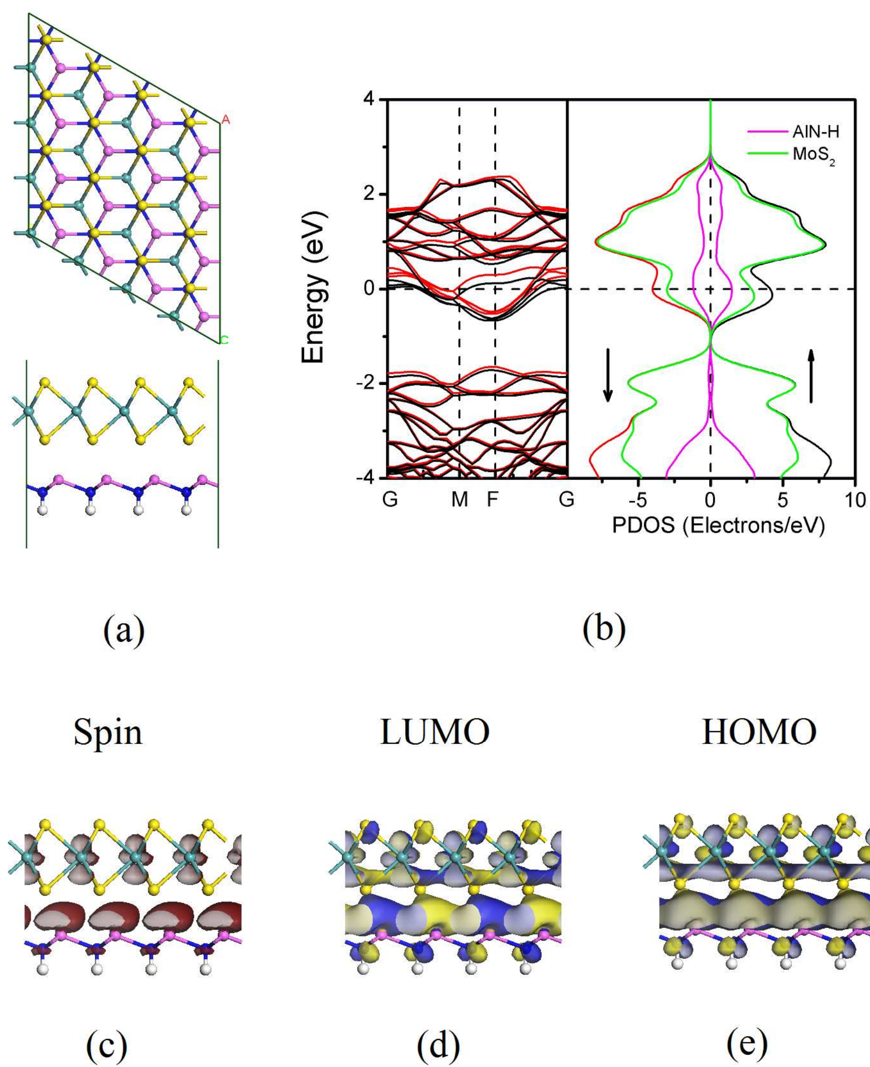

Physical Chemistry Chemical Physics Accepted Manuscript

Fig. 5

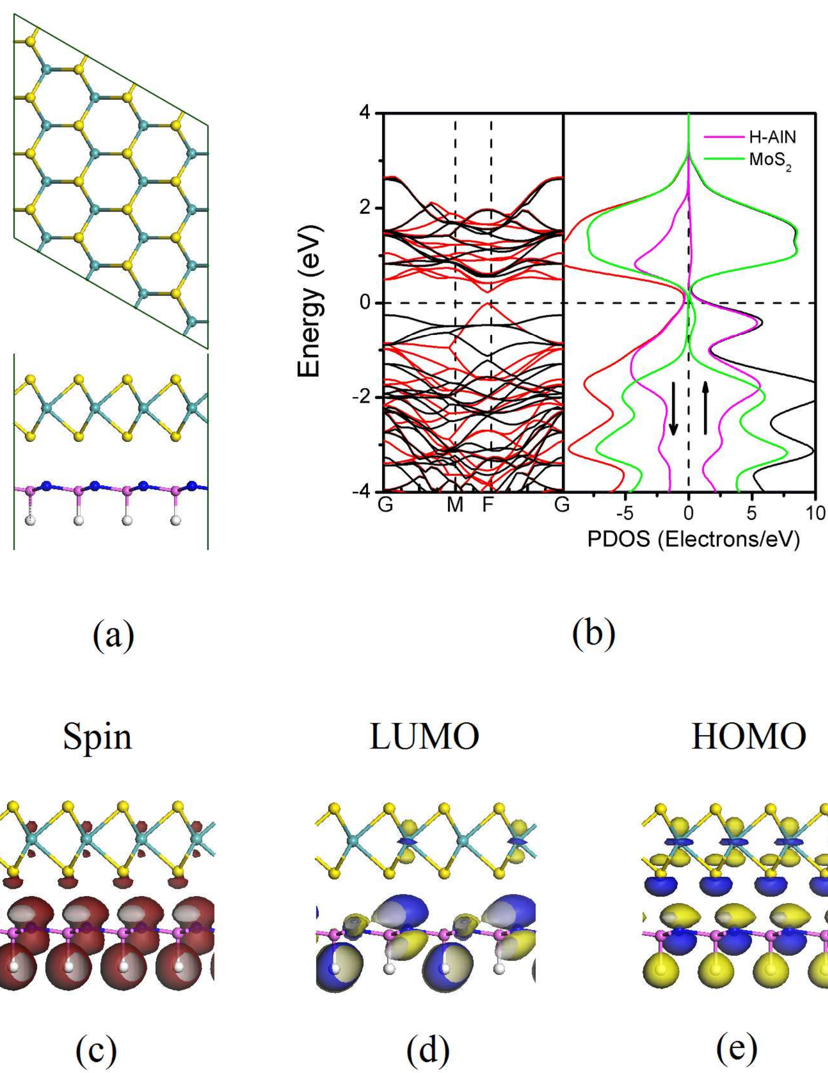

Physical Chemistry Chemical Physics Accepted Manuscript

Colour graphic

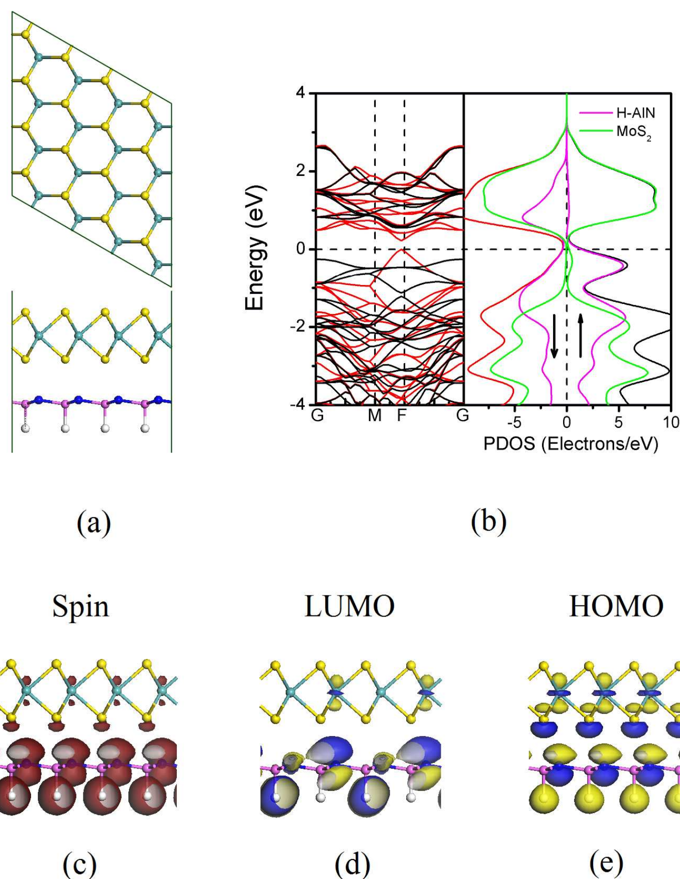

The structural, electronic, and magnetic properties of monolayer MoS_2 on decorated AlN nanosheets have been systematically investigated on density functional theory with van der Waals corrections. *n* type semiconductor → *p* type semiconductor → metal transition accompanied with nonmagnetic → magnetic transfer can be achieved for monolayer MoS_2 by surface microstructure of AlN substrate and stacking patterns.

Physical Chemistry Chemical Physics Accepted Manuscript